NASA TECHNICAL TRANSLATION NASA TT F 15,370

EXPERIMENTAL STUDY OF A WING PROFILE WITH FOWLER FLAPS AND SLATS

J. Barche

(NASA-TT-F-15370) EXPERIMENTAL STUDY OF A WING PROFILE WITH FOWLER FLAPS AND SLATS (Scientific Translation Service) 38 p HC $5.00 CSCL 01A

N74-17747

Unclas
G3/02 31460

Translation of "Experimental Studie an einem Profil mit Fowlerklappe und Vorflügel", DFVLR Papers on Fluid Dyn. with Emphasis on Boundary Layer Theory, Part 1. N73-33187 9 March 1972, pp. 7-44.

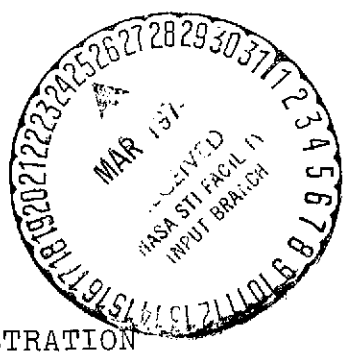

NATIONAL AERONAUTICS AND SPACE ADMINISTRATION
WASHINGTON, D. C. 20546 MARCH 1974

EXPERIMENTAL STUDY OF A WING PROFILE WITH FOWLER FLAPS AND SLATS *

Jürgen Barche

1. INTRODUCTION

/8 **

All the technical advances which have led to the development of faster aircraft could only be used in a restricted way if the take off and landing characteristics of the aircraft were noticeably reduced. This means that there is a parallel development of faster aircraft as well as a development of more effective high lift aids.

Usually experimental investigations of high lift aids are carried out, even though the test installations are such that the experimental results cannot be directly transferred. Therefore there were a large number of early papers which gave theoretical explanations of the flow mechanism. These were used to establish the flow in simple systems, for example [12], [2], [3], [4].

In the meantime, our knowledge of flow with and without friction has improved considerably, so that it even seems reasonable to deal with locally separated flow. Flows with local separation have become known as separation bubbles, especially at the leading edges of thin profiles, for example [5], [6]. However, they also occur in the gaps of flap profiles.

---

* Dedicated to Professor A. Walz on his 65th birthday.

** Numbers in the margin indicate pagination of original foreign text.

In this paper we will describe a few measurements carried out at the wind tunnel of the VFW-Fokker GmbH using profiles with high lift aids. The purpose of this report is to make a contribution to our theoretical understanding by analyzing known flow types. /9

2. NOTATION

c_a	Lift coefficient of the profile	$dA = c_a\, q_\infty\, l\, dy$
c_{as}	Lift coefficient of shock-free reentry	
c_m	Moment coefficient of the profile, positive tail heavy	$dM = c_m\, q_\infty l^2 dy$
c_{m25}	Moment coefficient around the 1/4 point on a profile	
c_p	Static pressure coefficient	$c_p = (p-p_\infty)/q_\infty$
c_{pt}	Total pressure coefficient	$c_{pt} = (p_t-p_\infty)/q_\infty = c_p + (v/v_o$
c_w	Drag coefficient of the profile	$dW = c_w\, q_\infty\, l\, dy$
h	Height coordinate of the perturbation zone normal to the profile	
h_a	Height of the separation zone	
h_∞	Height of the total pressure perturbation	
l	Profile chord	
l	Flap chord	
l_V	Slat chord	
p	Static pressure over the profile	
p_∞	Static ambient pressure	
p_t	Total pressure	
q_∞	Stagnation pressure of incident flow	
v	Local velocity	
v_∞	Incident velocity	
x	Longitudinal coordinate	

x_S	Longitudinal coordinate of the flap position (Figure 1)	
x_{SV}	Longitudinal coordinate of the slat position (Figure 1)	
y	Coordinate in the span direction	
z	Transverse coordinate	
z_S	Transverse coordinate of the flap position (Figure 1)	
z_{SV}	Transverse coordinate of the slat position (Figure 1)	
A	Drag	
M	Pitch moment, positive tail heavy	
Re	Reynolds number	$Re = v_\infty \, l/\nu$ /10
W	Drag	
α_g	Geometric angle of attack of the profile chord	
η_K	Flap deployment angle (Figure 1)	
η_V	Slat deployment angle (Figure 1)	

3. WIND TUNNEL, MODEL AND TEST DESCRIPTION /11

3.1. Wind Tunnel

The experiments described below were carried out in the wind tunnel of the VFW-Fokker GmbH. This is a tunnel of the Eiffel construction type with a test section of 2.1 x 2.1 m^2, a test section length of 4.5 m and a maximum velocity of 70 m/s ([7]). The test installation was installed in a chamber and has a mechanical six-component balance. The measured values can be evaluated on line using a process computer.

For profile measurements, a special test section is installed in the test section, which has a cross section of 1.0 x 2.1 m^2.

The profiles are mounted on rotatable disks, which can rotate without touching the walls of the special test section. These disks contain the suspension pins of the balances and the devices for automatically and remotely adjusting the flap parameters.

3.2. Model Geometry

The profiles measured in the VFW-Fokker wind tunnel basically have a width of one meter and the chord of 0.6 m for retracted flaps. At a velocity of 40 m/sec, this means that the Reynolds number is

$$Re = 1.6 \cdot 10^6$$

The investigations presented here are restricted to a measurement series using a basic profile having a Fowler flap and a slat. In order to characterize the profile geometry, the following key is used:

Profile	Meaning
A	Basic profile
B	Basic profile, Fowler flap 10°
C	Basic profile, Fowler flap 10°, Slat 30°
D	Basic profile, Fowler flap 1°
E	Basic profile, Fowler flap 40°

/12

Profiles A, B and C are shown in Figure 1 and were investigated in detail in this report. The coordinates of the basic profile of the Fowler flap and slat are shown in Table 1.

The basic profile belongs to the NACA laminar profiles see [8]. It was developed from profile NACA 63-A015 by a linear reduction to a relative thickness of 14.7%. The small degree of curvature was obtained by superposition of NACA central line a = 0.4 for the shock-free lift coefficient c_{as} = 0.11.

The Fowler flap has a Clark Y type profile. Its length l_k is 27% of the length of the basic profile l and the length of the slat is 14%.

The position of the Fowler flap is defined by the angle η_K between the wing chord and the flap chord and by the position of the flap nose x_s and z_s with respect to the effective trailing edge of the wing profile. The effective trailing edge with extended flaps is distinguished from the trailing edge of the basic profile by the so-called covering. As shown in Figure 1, this amounts to 97.5% of the wing chord along the top side of the basic profile. The position of the slat is given by the angle η_v between the leading edge chord and the wing chord and by the position of the slat trailing edge coordinates x_{sv} and z_{sv} relative to the nose of the basic profile. This is also shown in Figure 1.

Various gap coordinates given in the following table correspond to the various flap angles.

Profile	Gap coordinates					
	Fowler flap			Slat		
	η_k	x_s/l	z_s/l	η_v	x_{sv}/l	z_{sv}/l
A	-	-	-	-	-	-
B	10 °	-0.065	-0.035	-	-	-
C	10 °	-0.065	-0.035	30 °	-0.03	-0.03
D	1 °	-0.09	-0.04	-	-	-
E	40 °	-0.002	-0.014	-	-	-

3.3. Test Description

All the models were built so that forces, static pressure and some total pressures in the local wake could be measured. The test schedule is organized into three parts as follows: /13

- Force measurement
- Pressure distribution measurement and
- Wake measurement

The force measurement is done using a mechanical wind tunnel balance. The data are completely corrected on-line and are printed out as lift, drag and moment coefficients c_a, c_w and c_m, as well as in the form of the glide coefficient c_a/c_w. Therefore, it can be used to directly control the experiments. An automatic device makes it possible to adjust the flap gap during the operation, so that arbitrary gap coordinates can be preselected.

Automatic measurement point switching units are used for pressure distribution measurements. The signals are recorded on magnetic tape. The measurements are performed along the central line of the wing of the flaps and of the slat. Pressure distribution taps parallel to the incident flow direction are used to control the two-dimensional flow and in order to evaluate the wall influence of the special test section, especially at high lift values. All pressure measurement data are evaluated in the usual form of pressure coefficients c_p.

The weight measurements are performed using calibrated total pressure rakes. These rakes were developed to have a small directional sensitivity. The probe signals are also recorded on magnetic tape through automatic measurement point switching devices. The values are printed out as total pressure coefficients c_{pt}. The rakes are primarily installed at the flap trailing

edge, in the flap gap and in the vicinity of the leading edge.

4. RESULTS

4.1. Force Measurements

4.1.1. Definitions

By force measurements, we mean the determination of the lift, drag and moment coefficients c_a, c_w and c_m, from which further variables can be derived, such as for example c_a/c_w, the stability and the flap effectiveness. /14

All coefficients refer to the area of the wing having the basic profile and the chord 1. The changes of the wing chord by deploying the flaps are therefore absorbed in the coefficients. The 25% line is used as a reference point for the pitch moment. The Reynolds number of the experiment is $Re = 1.6 \cdot 10^6$.

4.1.2. Force Measurements over the Profiles

Figure 2 shows the coefficients c_a, c_w and c_m for the Profiles A, B, C and D, see Section 3.2 and Figure 1.

The coefficients for basic Profile A have the classical variation, i.e.

- The maximum lift is about c_{amax} 1.3 at $\alpha_{max} = 14°$
- The profile has trailing edge separation
- Nonlinear perturbations begin at $\alpha_g = 5°$
- Curvature lift or α_0-displacement correspond to the curvature line
- The zero moment caused by the curvature is slightly negative
- The profile is indifferent around the one quarter point and

drops off abruptly in a stable way.

The Profile D is produced from Profile A by deploying the Fowler flaps and by slightly rotating the flap to 1°.

In this way the effective wing chord is enlarged. The flap gap is widened and the wing curvature is increased. The results show these effects, that is / 15

- Increased inclination of the lift curve when referred to to the basic wing
- Increase in the curvature lift or the α_o displacement
- Increase of the maximum lift to $c_{a_{max}} = 1.96$
- At the same time decrease of the corresponding angle of attack to $\alpha_{max} = 13°$
- A state of flow which shows nose separation features.
- Intensification of the zero moment with
- Simultaneous increase in stability around the one quarter point of the basic profile for small lifts
- Small decrease in stability for large lift values below α_{max}
- Stable separation of the flow beyond α_{max}.

When the Fowler flap is extended further and primarily when it is rotated to the 10° position, we find profile B, which can correspond to a takeoff attitude of the flap (Figure 1). In addition to the effects already found in Profile D, which are intensified in this case, we find in particular that

- The maximum lift is increased to $c_{amax} = 2.5$

- The corresponding angle of attack $\alpha_{max} = 13°$ remains unchanged
- The increased load on the nose leads to leading edge separation

/ 16

If the slats are deployed in addition in order to stabilize the nose flow, see Figure 1, we find Profile C. The measurements clearly show the effect on the flow. It is characterized by the following:

- The lift increase is increased even more and
- The zero lift angle is displaced in the direction of positive angle of attack.

- The maximum lift is improved to about $c_{a_{max}} = 2.88$ and $\alpha_{max} 15°$
- The flow starts to separate along the nose, apparently here along the slat.
- The stability increases with increasing lift
- The wing becomes unstable below the maximum lift and it separates in an unstable way.

4.1.3. Glide Coefficients of the Profiles

The influence of the friction is more pronounced on the glide coefficient below the value of maximum lift. It has a greater influence than on the lift, drag and moment coefficients, shown in Figure 2. Figure 3 shows the glide coefficient c_a/c_w plotted against the lift coefficient as well as against the angle of attack.

We can observe the following.

- The best glide coefficient is about 46 and
- This is reached by the basic Profile A at $c_a = 0.5$ or $\alpha_g = 4°$.
- Above these values, the drag increase is considerably greater than the lift gain.
- The glide coefficients at $c_{a_{max}}$ are about the same, that is 18-20 for all profiles. / 17
- The slats only improve the flow above the lift coefficient $c_a = 2$ (see also Figure 2) and
- Below this value, it brings about considerable disturbances in the variation of the drag.

4.2. Pressure Distribution Measurements

4.2.1. Pressure Distribution of the Profiles

The following discussion of the pressure distributions is primarily restricted to Profiles A, B and C, which were shown in Figure 1.

The pressure coefficient c_p is shown, which describes the local static pressure over the profile compared with the surrounding pressure, and which was defined in Chapter 2. The pressures were recorded using automatic measurement point switches. They represent time average values as long as there are no low frequency fluctuations in the separation regions. Figure 4 shows these pressure distributions for Profiles A, B and C as a function of the longitudinal coordinate x/l. The angle of attack is the parameter for the curves. We selected a small and a medium angle of attack as well as an angle of attack in the vicinity of maximum lift.

The pressure distribution for basic Profile A again corresponds to a typical profile in this family. In particular, we can clearly observe that the pressure is constant along the

back part of the profile top side which is characteristic for a pure trailing edge separation. The maximum lift is therefore reached when the separation point indicating the beginning of constant pressure has penetrated to about the center of the profile.

The Profile B which is produced from the basic profile by extending and rotating the Fowler flaps by 10°, has a different structure of the pressure distribution. We can see that

- For comparable angles of attack, the flap induces considerable pressures along the wing.
- The flap induction brings about a loading of the profile nose.
- The pressure along the flap is only influenced slightly by the angle of attack.
- On the top side of the flap there is a collapse in the pressure which is apparently brought about because of covering by the profile (see Figure 1)
- Along the profile underside | and in the segment x/l = 0.7, there are regions of constant pressure which lead one to the conclusion that separation has occurred.
- The subsequent pressure increase indicates that the flow reattaches, that is, the separation bubbles amount to about 10 - 20% of the profile chord.

The pressure distribution in the flap gap is shown in Figure 7 on an enlarged scale. It will be discussed again in connection with the slat.

If the slat is extended from the profile and rotated by 30° then we obtain Profile C (see Figure 1). From the corresponding pressure distribution we find the following:

- The slat unloads the wing and takes over high underpressures along the top side.
- The flow along the slat under side is completely separated.
- For average angles of attack, apparently a separation bubble about 50 - 60% of the slat chord is produced.
- Only at angles of attack of about 15° does the stagnation point jump into the cutout along the lower side, so that a non-separated flow exists along the underside.
- The slat produces a similar collapse of the underpressure along the wing as was the case for the wing with the Fowler flap.
- There is no noticeable change in the rear part of the wing and along the flap, as compared with Profile B.

If the Fowler flap is extended from Position B even further and rotated to 40°, then we obtain Profile E, which could correspond to the landing position of this flap. The corresponding pressure distribution is shown in Figure 5 and shows the following:

- The maximum angle of attack was greatly reduced ($\alpha_{max} = 7°$, $c_{a_{max}} = 3.2$)
- The wings as well as the flap have separations at the trailing edges at small angles of attack.
- There is no collapse of the underpressure along the flap top side.
- The influence of the angle of attack on the flap pressure distribution is small.

4.2.2. Flow Conditions for the Basic Profile

In Figures 4 and 5 we show the pressure distributions in the usual way. A new way of representing this is shown in Figure 6. In this case, the pressures at a few measurement points along the top side of the basic Profile A were traced as a function of

angle of attack. It can be seen that at each measurement point there are apparently three different flow states, depending on the angle of attack, which each have the following regions: /20

- Linear region
- Nonlinear region
- Separated region

In the linear region, the underpressure increases linearly with angle of attack and the friction apparently does not play an important role. The increase and the width of the region along the front part of the profile is greater than for the rear part.

The separated region represents the part of the profile over which there is trailing edge separation. Since here there is approximately constant pressure, the pressures of all influenced profile parts coincide. The separated region advances in the direction of a profile nose as an angle of attack is increased, and the underpressure first increases further.

The transition from a linear region to the separated region is carried out in the nonlinear transition phase. Accordingly, this is a phase in which the pressure distribution is influenced by the separations which are downstream, but the separation has not yet reached the corresponding point. Figure 6 shows that the linear state ends at 11° at the one-quarter point of the profile. The separation has advanced to about 90% of the profile chord. In the separated region, the underpressure is $c_p = 0.2$. The one-quarter point is also reached by the separation at about 16°. The underpressure in the separated field is then increased to $c_p = 0.65 - -0.7$

4.2.3. Pressure Distribution in the Flap Cutout

The pressure distribution in the flap region of the Profile B is again shown in Figure 7 with an enlarged scale. If the pressures along the under side of the wing before and after the flap cutout are plotted against the angle of attack, we find the variation shown in Figure 8. Since the pressures in the flap cutout at x/l = 0.72 in any case belong to a region of separated flow, we find a relationship between the separated flow and the flap cutout and the non-separated flow ahead of the cutout. We find the following. / 21

- Here again we must distinguish three flow regions, which can be divided into a linear, nonlinear and separated region.
- In the linear region, the overpressure of a separated flow as well as the overpressure of the non-separated flow increase linearly with angle of attack.
- In the nonlinear transition region, the pressures ahead of and inside of the flap cutout approach each other gradually so that
- They coincide in the separated region, because the separation begins already before the cutout and the
- The overpressure decreases rapidly when angle of attack is increased further.

4.2.4. Pressure Distribution in the Slat Cutout

It is natural to investigate the flow conditions along the underside of the slat for similar effects. It is advantageous that the distance between the stagnation point and the separation point be relatively small.

Let us consider Figure 9. It shows the pressure distribution along the slat under side for a small, average and large angle of attack. We find different pressure distributions for each of these angles of attack.

For small angles of attack, the stagnation point lies along the top side of the slat (see Figure 4). The streamline directed to the under side therefore surrounds the slat nose and separates at the cutout. This separation apparently occurs without subsequent reattachment.

For average angles of attack, the stagnation point already /22
lies in the vicinity of the slat cutout. Here again the flow separates but reattaches later on. This can be seen from the pressure increase at the end of the slat. Just like in the cutout of the Fowler flap and in contrast to the thin wing profile, we again find an overpressure in the separation bubble.

It is only at larger angles of attack that the stagnation point jumps into the slat cutout. In this case, the slat lower side does not have any flow separation which is visible. A separation bubble is suspected to occur along the top side, however. The pressure distribution shown in Figure 4 indicates this. This bubble does not influence the lift much but does substantially influence the overall drag because of the reduced nose thrust.

Let us consider the pressure distribution at two measurement points of the slat lower side as a function of angle of attack. Here again we find the three different flow states. The pressure can either:

- Not change with angle of attack, as long as the flow does not reattach again.
- Decrease linearly with angle of attack, if the separation bubble closes again.
- Obey the laws of non-separated flow, as soon as the stagnation point has jumped into the slat cutout.

4.3. Wake Measurements

4.3.1. Definitions

Rakes were used for the wake measurements. To begin with, they are independent of the flow direction over a large angular range, and they can be calibrated. The total pressure is described by the coefficient c_{pt} which indicates the change in the local total pressure compared with the static pressure of the surroundings, and which is referred to the stagnation pressure of the incident flow (see Chapter 2).

If the rake indicates the value $c_{pt} = 1$, then the flow has reached the measurement point without any losses. $c_{pt} = 0$ indicates a pressure loss equal to the stagnation pressure magnitude. For the flow around a flat plate, this is an indication of the beginning of separation. For flows around arbitrary contours, the separation only occurs for negative indications of total pressure.

The total pressure rake does not give any useful signals for the reverse flows in separation regions. The limits of negative indications which can be evaluated can be estimated as follows. In the separation zones, the average flow velocity must be relatively small, so that the rake will give approximately a constant indication over the entire height of this zone, which is of the order of the static pressure.

4.3.2. Wake Measurements along the Profile Trailing Edges /23

Figure 10 shows the measurements of the total pressure in the wake of Profiles A, B and C. The angles of attack shown as parameters are approximately those used for the pressure distribution measurements. The rake was attached to the trailing edge of the profile or to the Fowler flap.

The measurement for the basic Profile A shows clearly that

- The profile curvature results in various loss regions along the top side and the bottom side for incident flow parallel to the chord.
- The losses are displaced to the top side with increasing angle of attack.
- The height of the loss zone amounts to about 7-8% of the profile chord at maximum angle of attack.
- In a negative region, constant readings are obtained over a height of 3%.
- These indications are a measure for the height of the separation zone along the trailing edge. / 24

If we compare these results with those for Profile B, we find the following influence of the flap gap.

We can see that:

- The pressure flow of the flap gap brings about a reduction in the loss.
- The separations in the flap cutout determined from the pressure distributions are certainly the reason for the remaining gap losses.

- Separations in the wake of the gap do not occur. Therefore the flow in the flap cutout must have reattached in the form of a bubble.
- There are strong pressure losses along the back side of the flap.
- There are large losses from the top side of the profile as angle of attack is increased
- For maximum angle of attack, there are no indications of trailing edge separation.

If the slat is extended from Profile B and rotated by 30°, we find Profile C. The corresponding wake measurement shows that

- The flow perturbation through the flap gap and in its surroundings is great at small angle of attack.
- This is due to the perturbations along the profile under side and upper side caused by the slat.
- A strong wake is produced by the top side of the slat at maximum angle of attack.

The height of the loss region h_∞ and the height of separation h_a are shown in Figure 11 for the basic Profile A as a function of angle of attack. The figure does not give any indication of the drag distribution along the profile top side and bottom side. However, it does give an indication of the range of the perturbation with increasing angle of attack.

For a Reynolds number of Re = $1.6 \cdot 10^6$ and a maximum lift /25
of the profile, accordingly the total pressure perturbation along the top side can amount to 8% of the profile chord, and to less than 1% along the under side. The corresponding height of the reverse flow zone is about 3%.

4.3.3. Wake Measurements in the Vicinity of the Profile Leading Edge

The total pressure profiles shown in Figure 10 indicate perturbations which have already occurred along the wing's leading edge. This can be seen from Figure 12 which shows measurements along the top side of the wing with a backward displacement of about 15% of the chord.

Up to an angle of attack of 8°, there is no perturbation in the vicinity of the leading edge for the basic Profile A. If the incidence is increased further, a flat "loss tongue" enters the undisturbed flow, which can be identified with the beginning of the nonlinear region shown in Figure 6.

Similar conditions can also be found for Profile B. The loss tongues already occur at smaller angles of attack, because the deployment and rotation of the landing flap to 10° brings about a greater loading of the profile nose (see Figure 6). By extending the flap further, Profile C is produced from Profile B. The flap has a strong influence on the flow around the nose region. The influences already shown in Figure 9 can be found here again. Figure 12 shows the following:

- For small angles of attack there is a total pressure perturbation along the wing top side caused by separated flow along the under side of the slat.
- For average angles of attack the flow has no losses, directly on the profile top side. The slat perturbation lies above it at a height of about 1% of the profile chord.

- For larger angles of attack, there is a strong perturbation /26 caused by separation along the slat top side at a height of 1.5 - 2% of the wind chord above the profile (see Figure 15).

4.3.4. Wake Measurements in the Flap Gap

Wake measurements inside and above the flap gap are shown in Figures 13 and 14 for Profiles B and C. Figure 13 corresponds to Profile B and shows the following:

- The gap losses become smaller with increasing angle of attack.
- The gap flow has no losses directly on the flap.
- The losses must increase rapidly above the flap length (see Figure 10).
- The gap losses are primarily due to the separation bubble region (see Figure 7).
- The total pressure losses along the profile top side increase with angle of attack and
- They are greater than those in the flap gap.

Similar tendencies are found in corresponding measurements with Profile C, i.e., for the extended slat (Figure 14). In this case, there is also a parallel displacement of the total pressure profiles in the flap gap. This displacement is produced by the perturbation to the slat along the lower side of the wing at small and moderate angles of attack.

5. SUMMARY /27

This study describes force, pressure distribution and wake measurements carried out with a two-dimensional basic profile having Fowler flap and slats in the wind tunnel of the VFW-Fokker GmbH. All measurements were carried out in a special

test section of the tunnel with a Reynolds number of

$$Re = 1.6 \cdot 10^6$$

The purpose of the report is to give an experimental analysis of the flow conditions for locally attached and separated flow in order to make contributions to future theoretical work. The experimental results have been presented in a classical way, and special graphical techniques have been used for the separated flow regions.

/ 28

REFERENCES

1. Multhopp, H. Calculation of Lift Distribution of Lifting Surfaces. Lufo, Vol. 15, 1938.

2. Jordan, D. Lift Calculations and Flow Processes when Maximum Lift is Exceeded. Lufo, Vol. 16, 1939.

3. Walz, A. Calculation of the Pressure Distribution over Flap Profiles with Dead Water Regions. Lufo, Vol. 17, 1940.

4. Walz, A. Theoretical Calculations of the Maximum Lift Coefficient of Wind Profiles With and Without Lifting Flaps. Forsch. Ber.d.Z.f.wiss.Ber.. - Wesen FB 1769, 1943.

5. Prandtl, L. Führer durch die Strömungslehre (Guide to Fluid Dynamics). Verlag F. Nieweg u. Sohn, Braunschweig 6th Edition, Chap. 7.1.1, 1965.

6. Tani, I. Progress in Aeronautical Sciences. Vol. 5, 1964.

7. Ewald, B. Wind Tunnel of the VFW-Fokker BmbH. Ea-Short Report, Not Published.

8. Abbott, I., and A. Doenhoff v. Summary of Airfoil Data. NACA-Rep. 824, 1945

TABLE 1. REMARK: COORDINATES ARE REFERRED TO A PROFILE SKELETON LINE WHICH IS INCLINED TO THE PROFILE CHORD BY 0.5° *

1. Base profile

Top side		Lower side	
$\bar{x}/l$	$\bar{z}/l$	$\bar{x}/l$	$\bar{z}/l$
0	0,00218	0	0,00218
0,00426	0,01431	0,00574	-0,00926
0,00675	0,0169	0,00825	-0,01152
0,01162	0,0212	0,01338	-0,01515
0,0240	0,0288	0,02595	-0,02184
0,0492	0,0398	0,0510	-0,0312
0,0742	0,0482	0,0759	-0,0382
0,0995	0,0546	0,1050	-0,0435
0,1245	0,0602	0,1245	-0,0475
0,1450	0,0648	0,150	-0,0519
0,1750	0,0688	0,1749	-0,0553
0,202	0,0720	0,1995	-0,0581
0,225	0,0746	0,2495	-0,0625
0,250	0,0769	0,2996	-0,0652
0,276	0,0785	0,3495	-0,0665
0,326	0,0806	0,3996	-0,0661
0,375	0,0806	0,450	-0,0645
0,425	0,0788	0,4999	-0,0618
0,475	0,0753	0,550	-0,0582
0,525	0,0704	0,600	-0,0537
0,575	0,0642	0,650	-0,0485
0,625	0,0572	0,700	-0,0428
0,675	0,0492	0,750	-0,0368
0,725	0,0408	0,800	-0,0308
0,775	0,0323	0,850	-0,0248
0,825	0,0237	0,900	-0,0189
0,875	0,0152	0,950	-0,0129
0,925	0,00666	1,00	-0,00696
0,975	-0,00185		
1,00	-0,00612		

Nose radius $r/l = 0.0164$

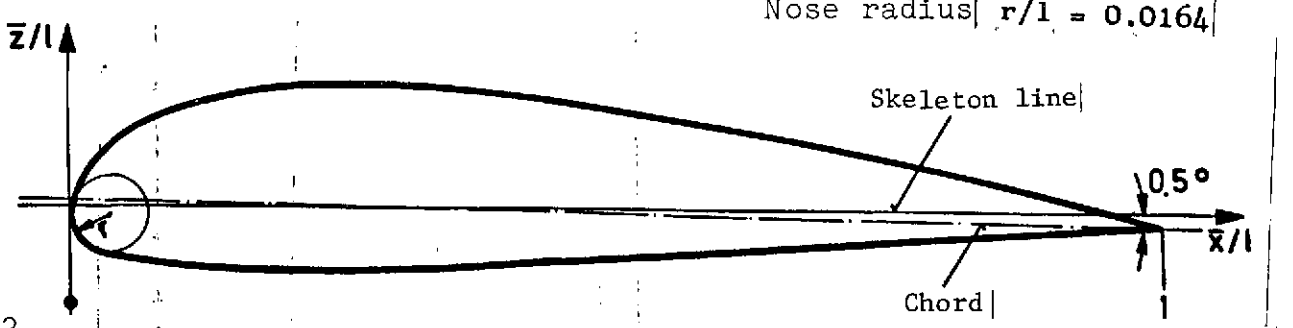

* Translator's note: Commas in numbers represent decimal points.

TABLE 1 (CONTINUED)*

2. Slat contour

$\bar{x}/l$	$\bar{z}/l$
0,0229	-0,0148
0,0268	-0,00812
0,0308	-0,00230
0,0349	+0,00290
0,0392	0,00765
0,0435	0,01195
0,0478	0,0161
0,0556	0,0232
0,0656	0,0297
0,0746	0,0355
0,0840	0,0407
0,1220	0,0566
0,1460	0,0635
0,1558	0,0656
0,1603	+0,0665

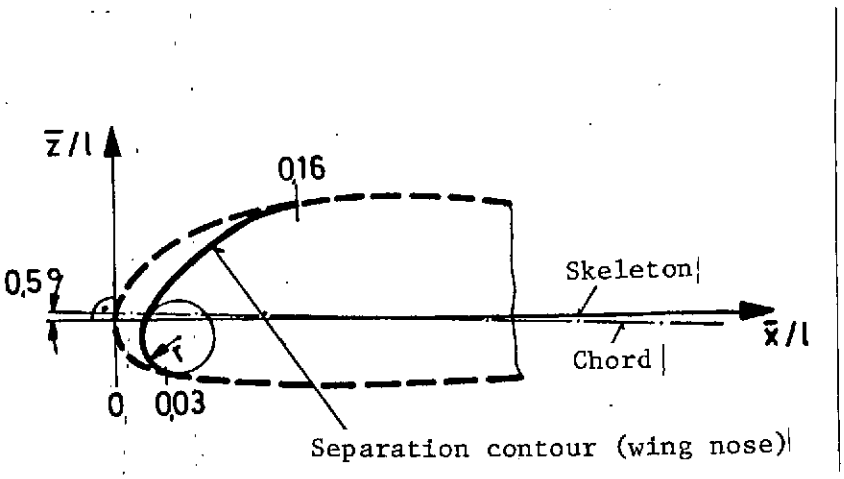

Nose radius r/l = 0.0988

3. Flap contour

$\bar{x}/l$	$\bar{z}/l$	
0,7180	-0,0300	Top side
0,7237	-0,0182	
0,7347	-0,0109	
0,7592	+0,0011	
0,8005	0,0064	
0,8037	0,0068	
0,8422	0,0092	
0,8812	+0,0084	
0,7167	-0,0313	Nose point
0,7211	-0,0376	Lower side
0,7248	-0,0389	
0,7320	-0,0389	

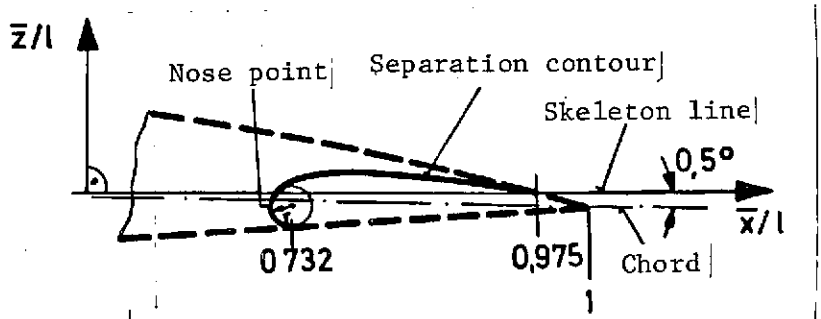

Nose radius r/l = 0.007

* Translator's note: Commas in numbers represent decimal points.

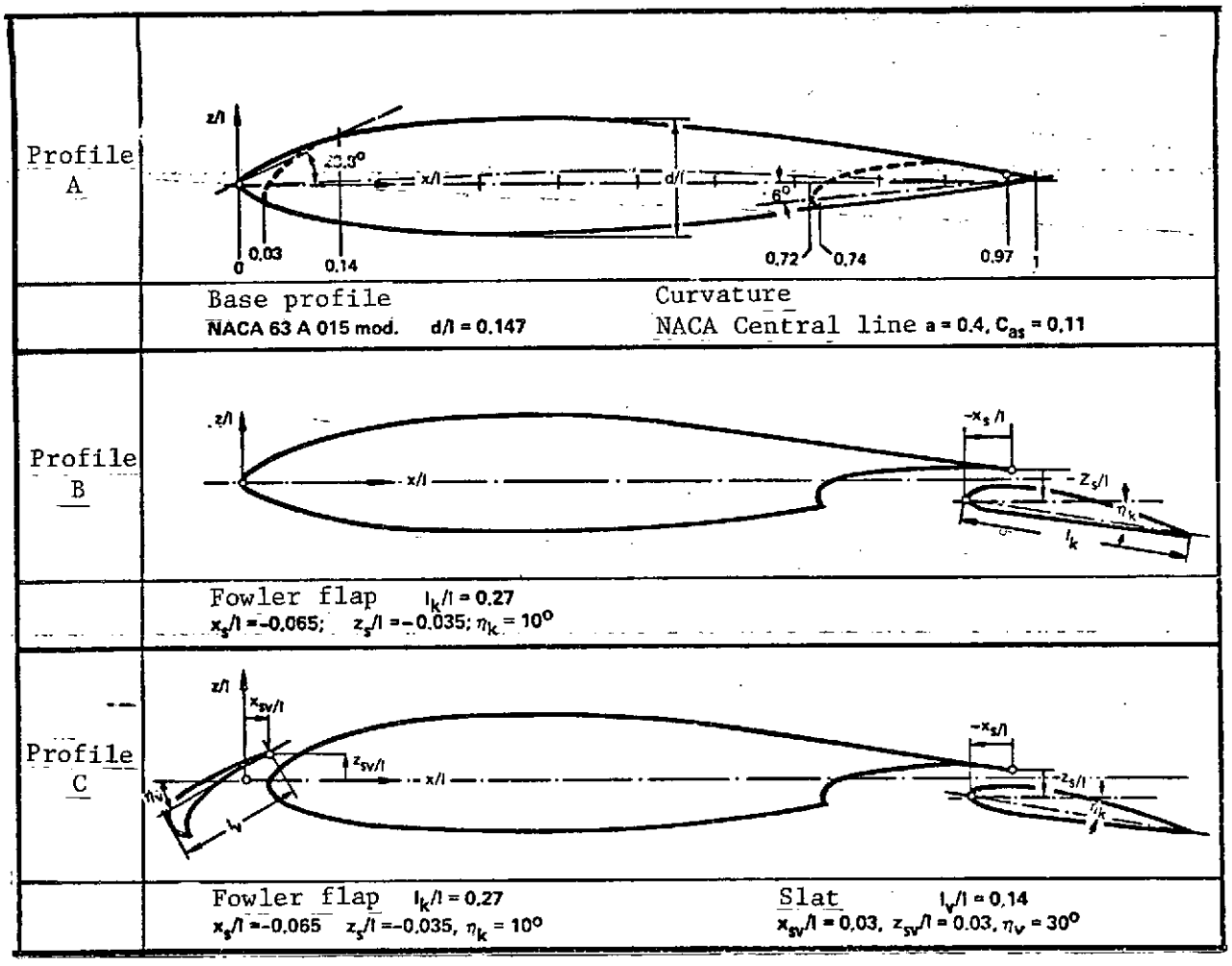

Figure 1. Profile geometry.

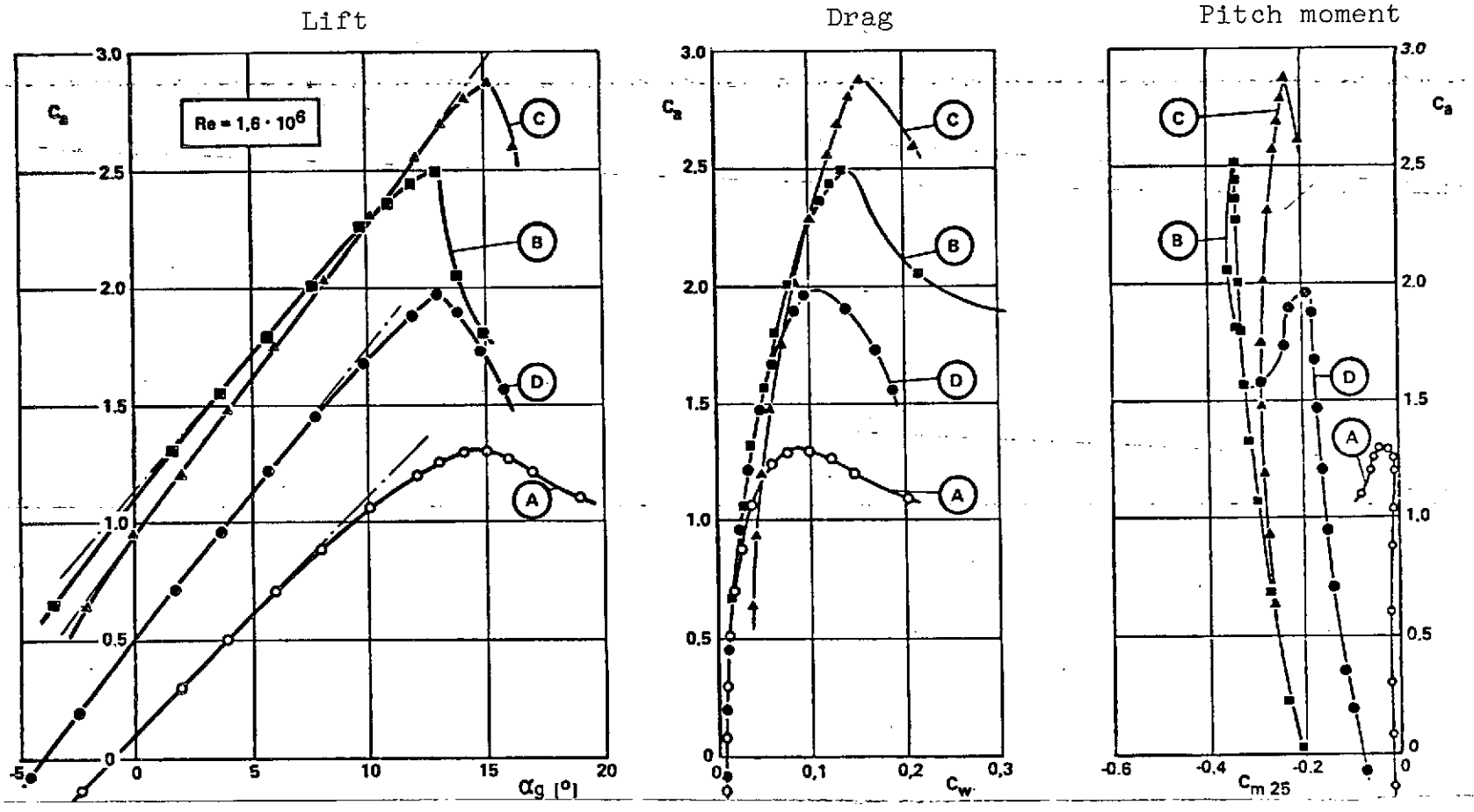

Figure 2. Force measurement. Lift, drag, pitch moment.

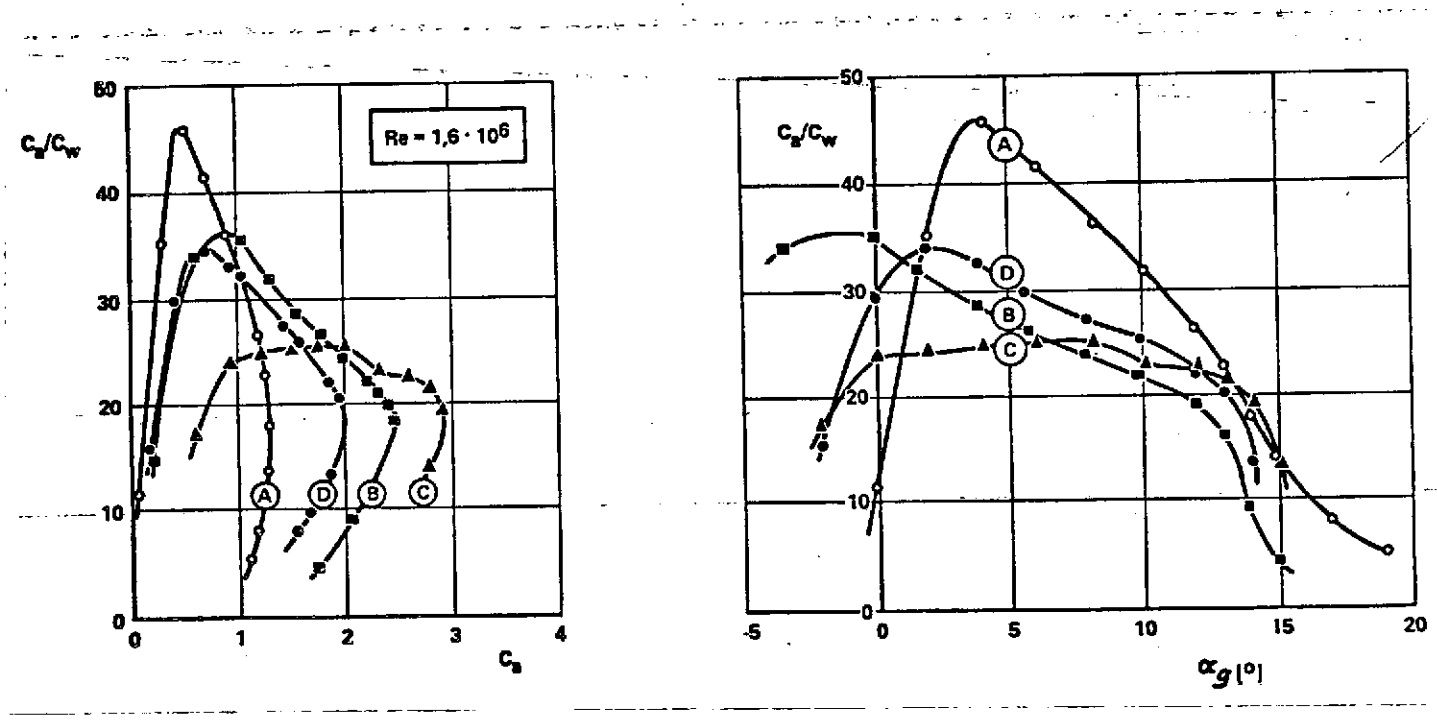

Figure 3. Force measurement. Glide coefficient.

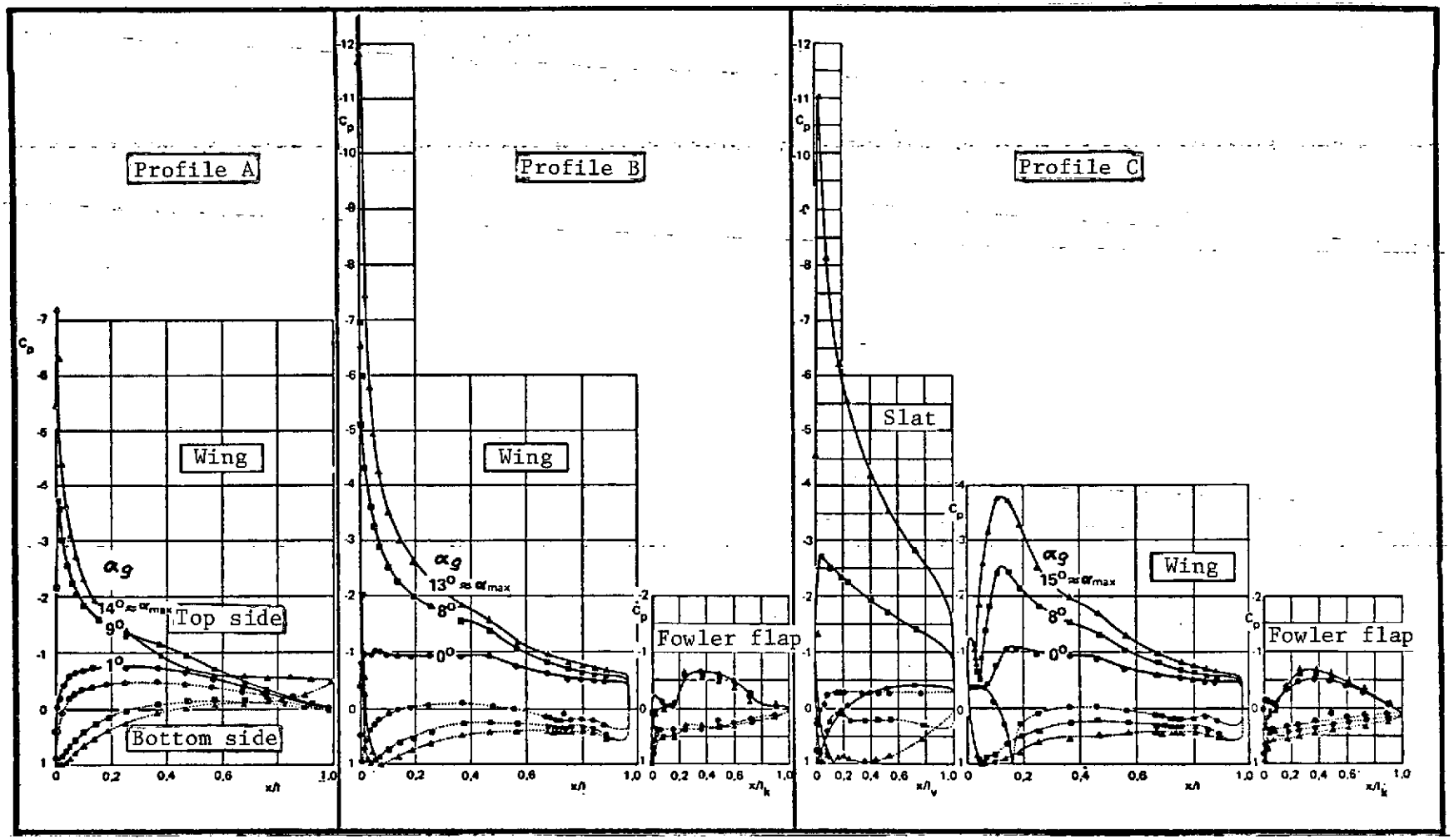

Figure 4. Pressure distribution measurement. Profiles A, B and C.

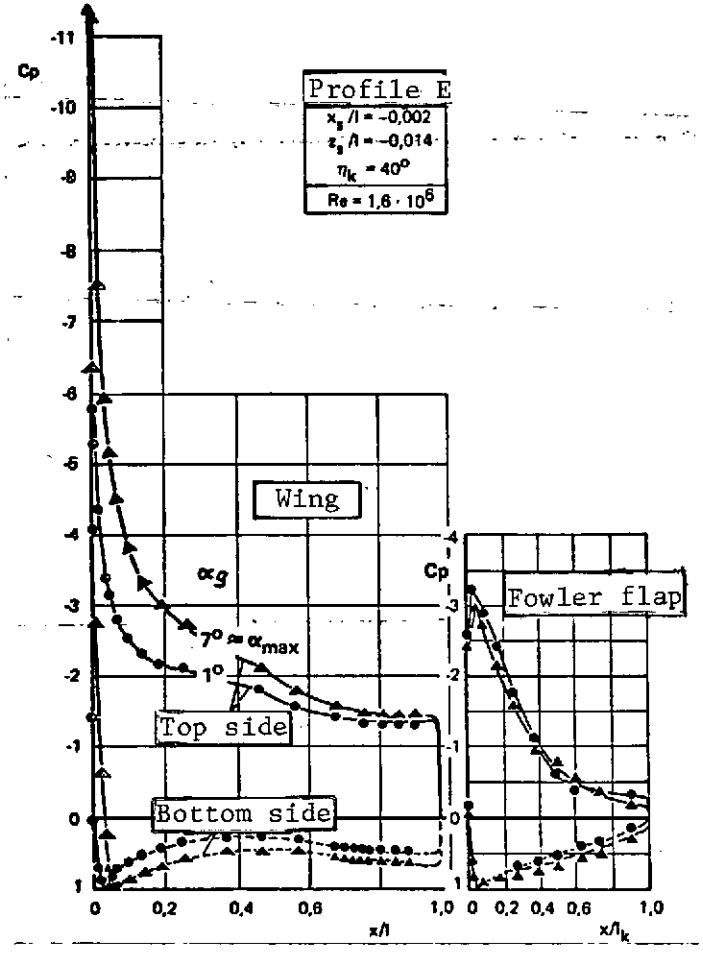

Figure 5. Pressure distribution — measurement. Profile E.

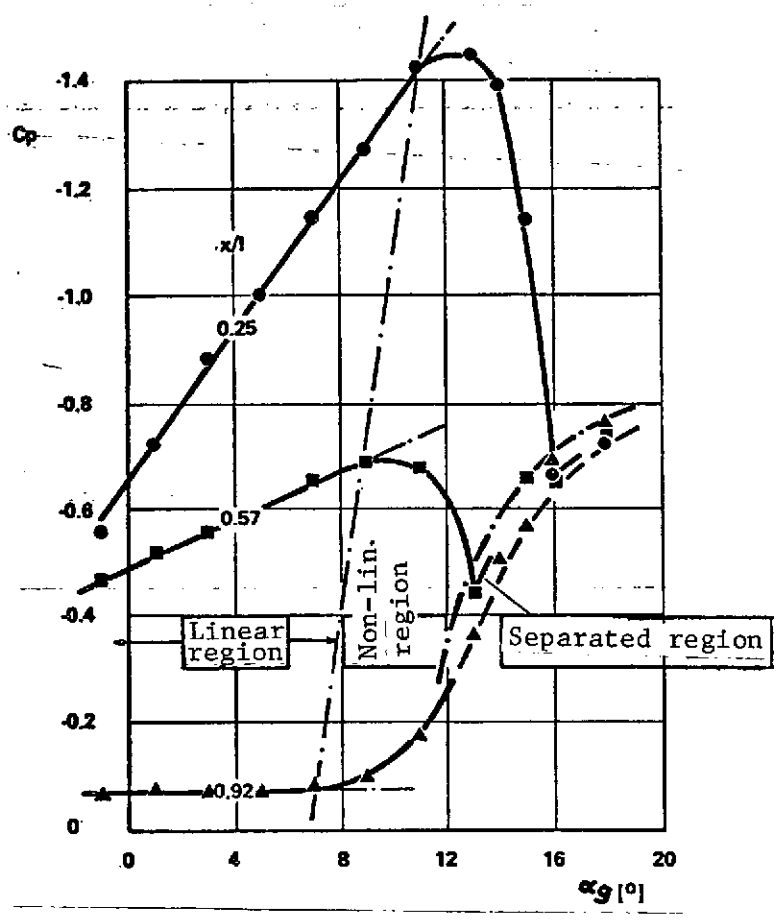

Figure 6 Pressure distribution measurement. Profile A, Top side

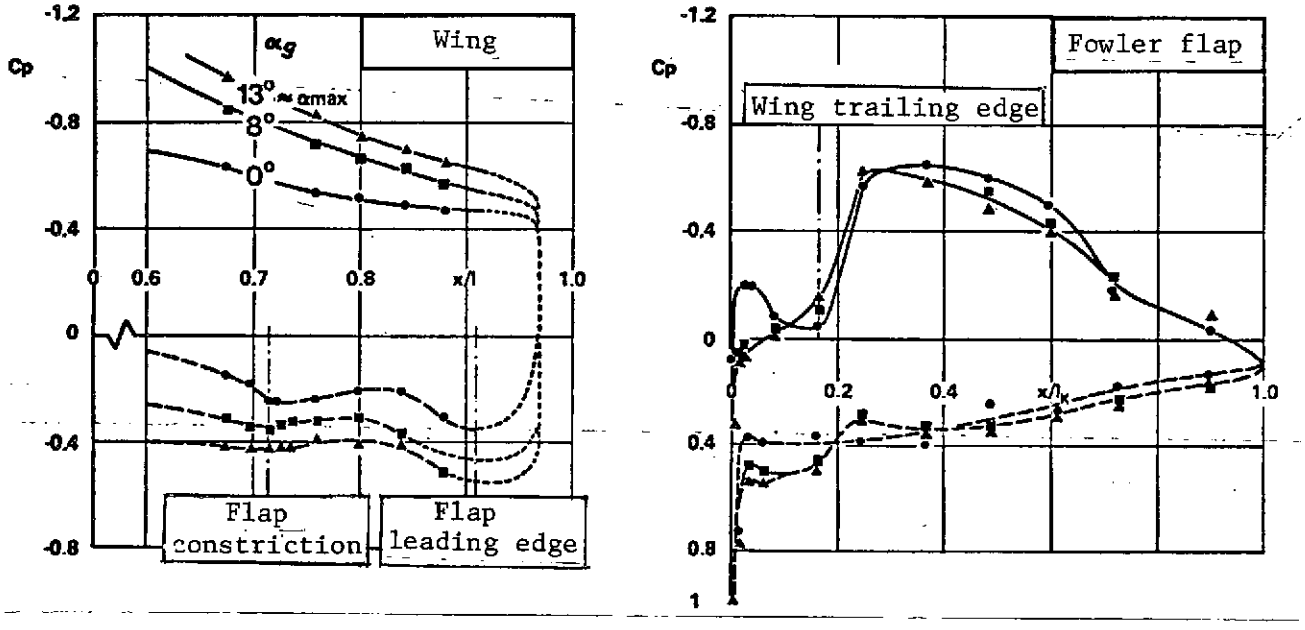

Figure 7. Pressure distribution measurement. Flap region profile B

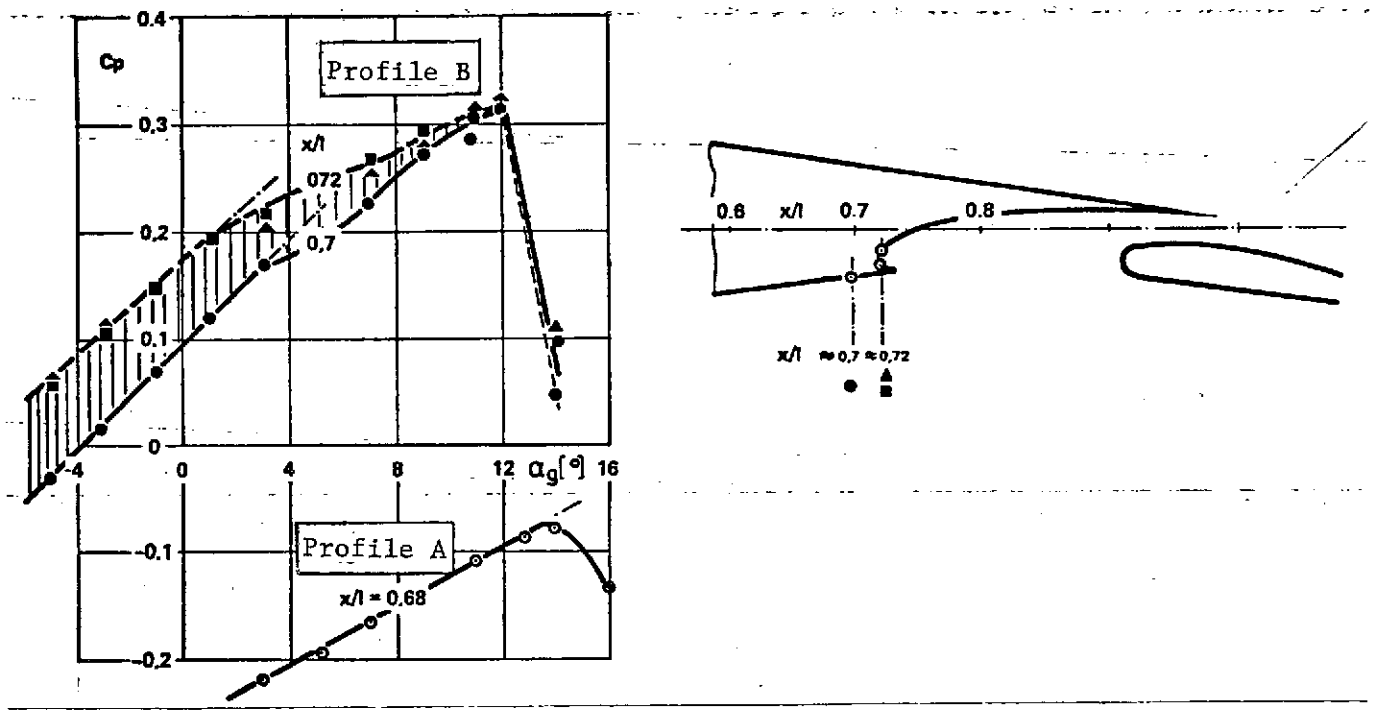

Figure 8. Pressure distribution measurement. Pressure at the flap constriction.

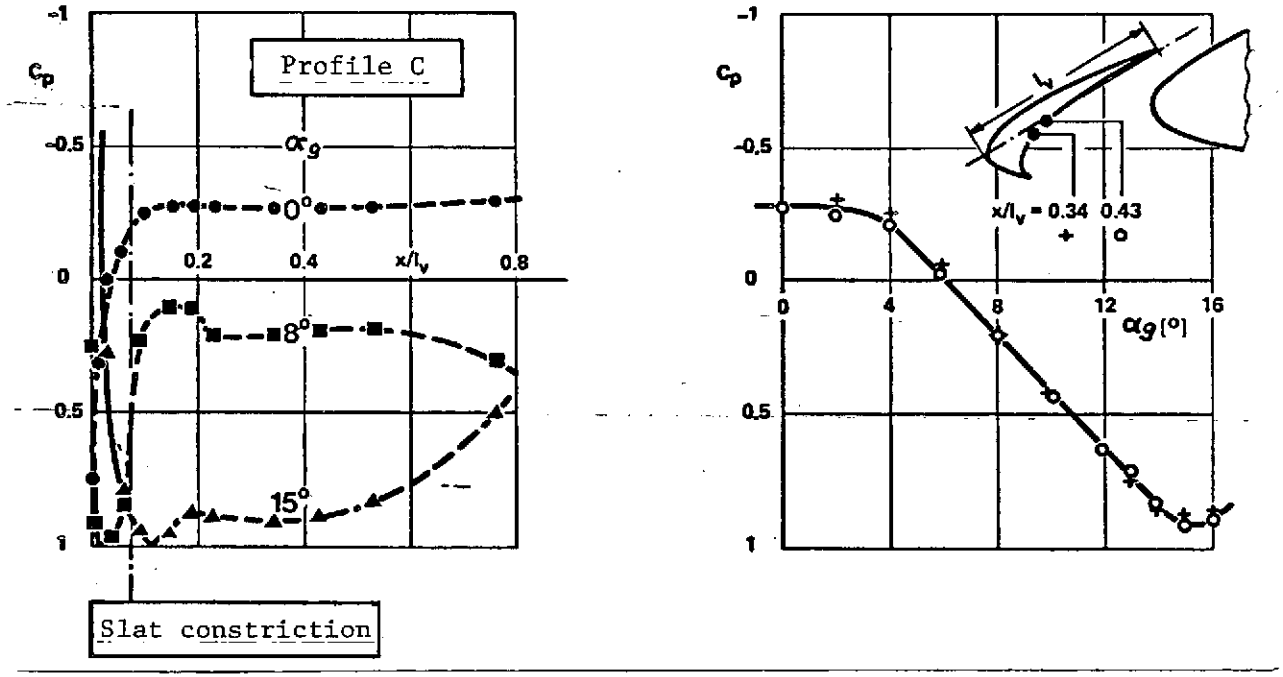

Figure 9. Pressure distribution measurement. Pressure along slat lower side.

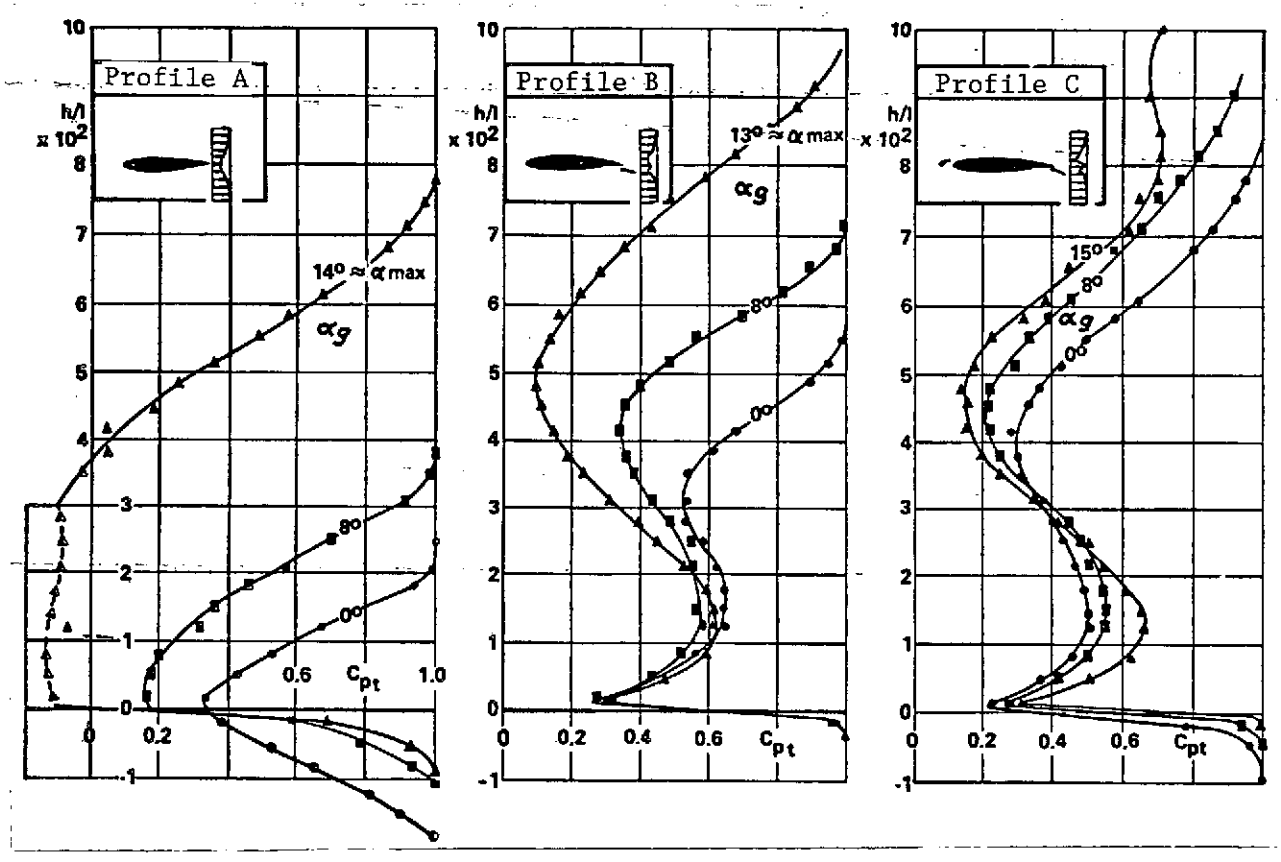

Figure 10. Wake measurement. Trailing edge.

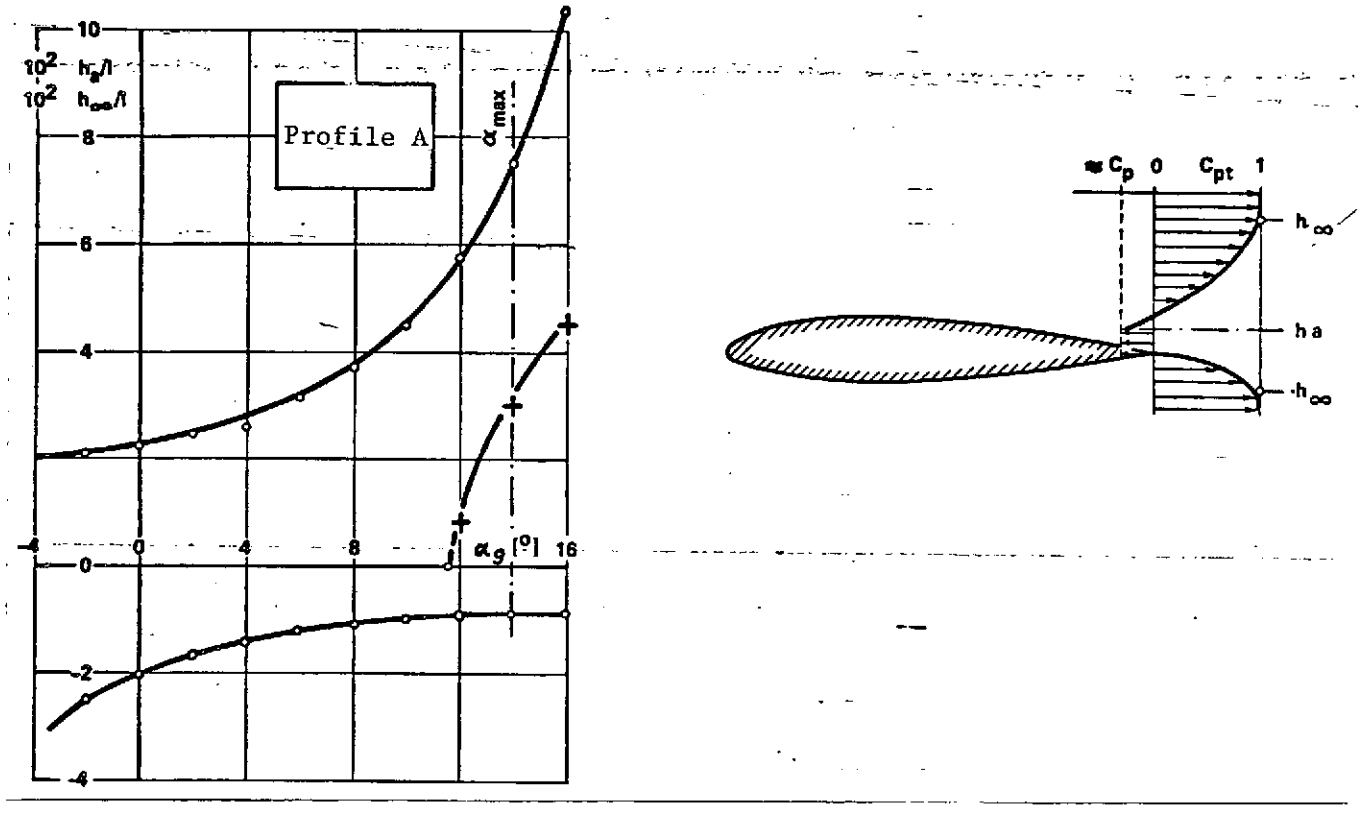

Figure 11. Wake measurement. Wake height.

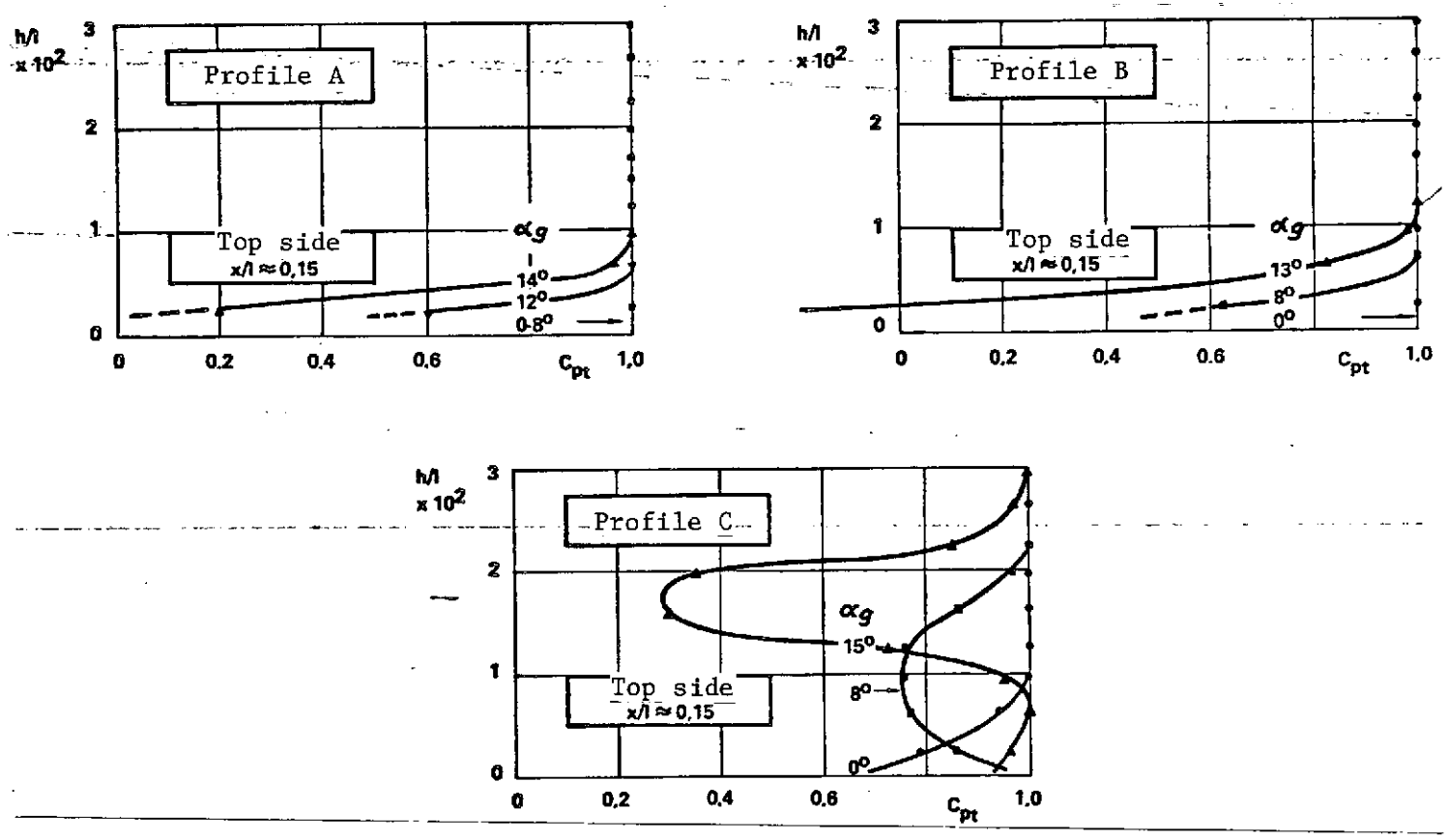

Figure 12. Wake measurement. Profile nose, top side.

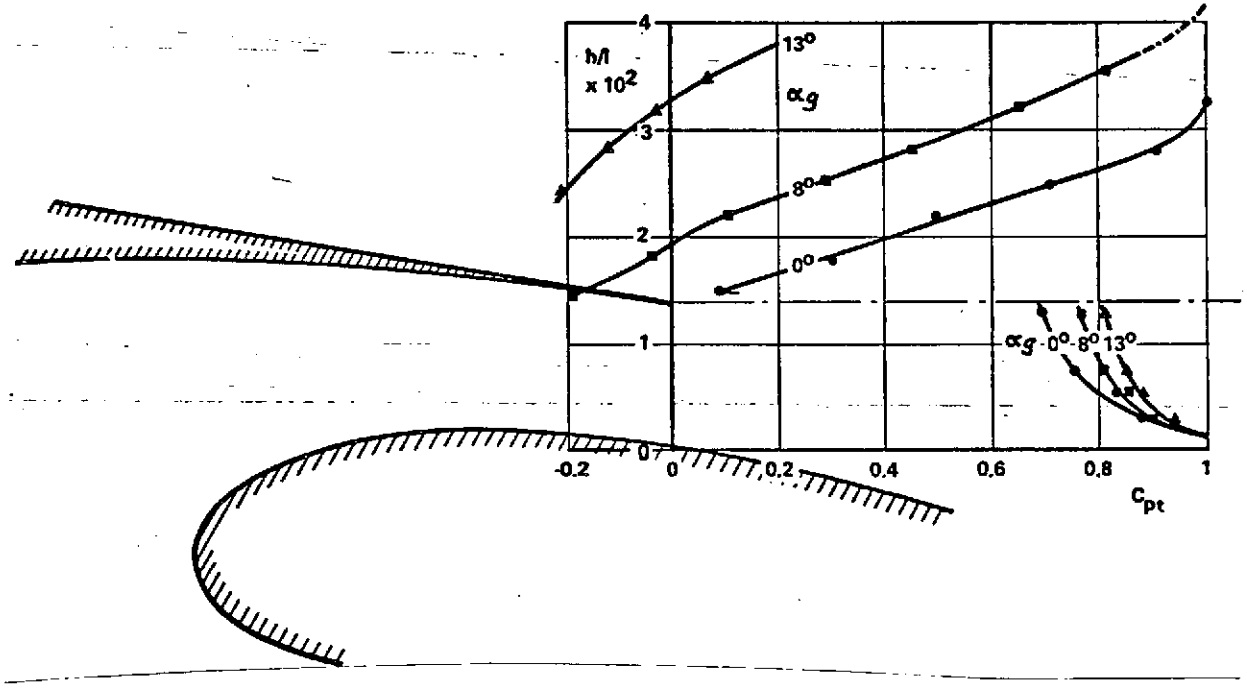

Figure 13. Wake measurement. Flap gap.

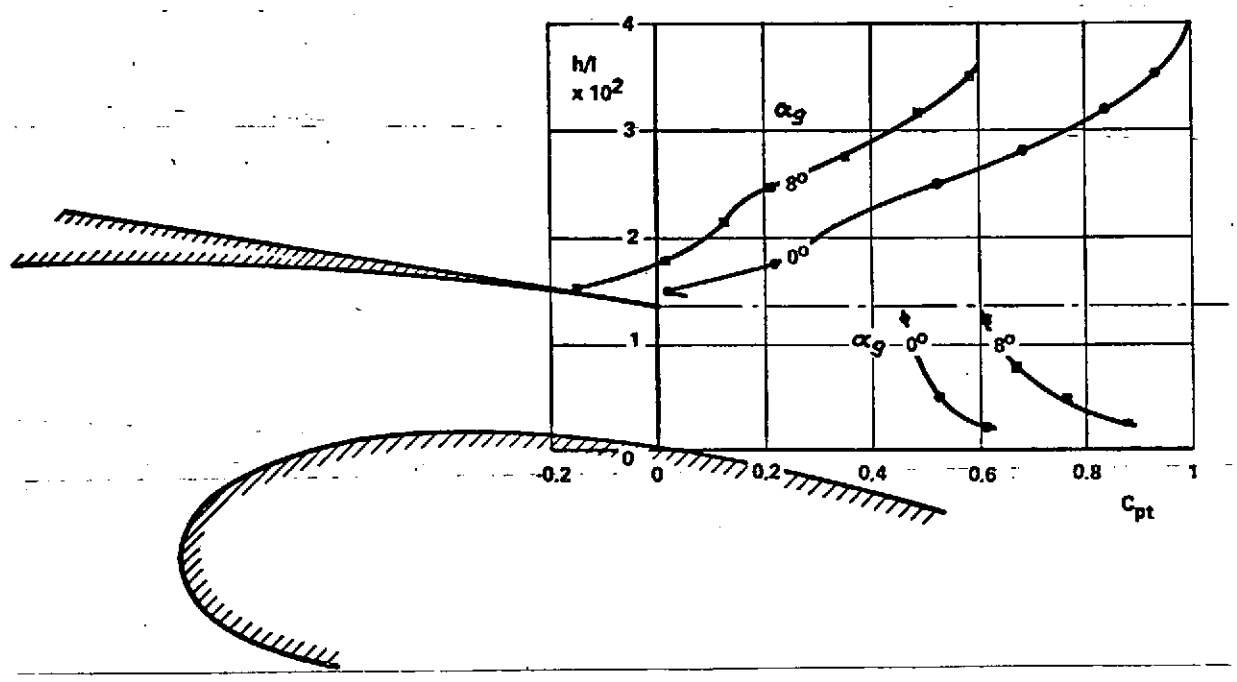

Figure 14. Wake measurement. Flap gap.

STANDARD TITLE PAGE

1. Report No.	2. Government Accession No.	3. Recipient's Catalog No.
NASA TT F- 15,370		

4. Title and Subtitle	5. Report Date
EXPERIMENTAL STUDY OF A WING PROFILE WITH FOWLER FLAPS AND SLATS	March, 1974
	6. Performing Organization Code

7. Author(s)	8. Performing Organization Report No.
J. Barche	10. Work Unit No.

9. Performing Organization Name and Address	11. Contract or Grant No.
SCITRAN Box 5456 Santa Barbara, CA 93108	NASw-2483
	13. Type of Report and Period Covered
	Translation
12. Sponsoring Agency Name and Address National Aeronautics and Space Administration Washington, D.C. 20546	14. Sponsoring Agency Code

15. Supplementary Notes

Translation of "Experimental Studie an einem Profil mit Fowlerklappe und Vorflügel". DFVLR Papers on Fluid Dyn. with Emphasis on Boundary Layer Theory, Part 1, N73-33187 9 March 1972, pp. 7-44.

16. Abstract

Usually high lift aids for aircraft are examined on scale-down models. The application of this experimental data is problematical. There is a basic interest in establishing a theory for the flow conditions over the flap system during takeoff and landing. The present experimental study attempts to provide the basis for future theoretical models based on detailed measurements over a simple profile which has Fowler flaps and slats.

17. Key Words (Selected by Author(s))	18. Distribution Statement
	Unclassified - Unlimited

19. Security Classif. (of this report)	20. Security Classif. (of this page)	21. No. of Pages	22. Price
Unclassified	Unclassified	38	